

KAYAK PERFORMANCE MODELLING USING SPH

Simon M. HARRISON^{1*}, David F. GUNN¹ and Paul W. CLEARY¹

¹ CSIRO Mathematics, Informatics and Statistics, Clayton, Victoria 3168, AUSTRALIA

*Corresponding author, E-mail address: Simon.Harrison@csiro.au

ABSTRACT

Kayak racing performance is known to be dependent on both technique and strength, but the relationship between these attributes and performance is not well understood. Complete experimental measures of stroke technique and the interactions between the water and the paddle and the boat are not practical in the racing environment. Instead, simulation using computational fluid dynamics may be used to study this system. A coupled biomechanical-Smoothed Particle Hydrodynamics (SPH) model of the kayaking athlete is presented. Using stroke technique digitised from video of an amateur level athlete and literature data, calculations are made of (a) the fluid response to interactions with the paddle and kayak; (b) six degrees of freedom kayak motion; and (c) magnitudes of blade force and impulse. Key features of the fluid response are related to the loading on the athlete and the speed of the kayak. Perturbations to stroke technique are explored to give new insights into the relationships between technique and racing performance.

INTRODUCTION

Kayak racing performance depends on athlete attributes such as aerobic and anaerobic capacities (Bishop, 2000), anthropometry (van Someren and Palmer, 2003), strength and stroke technique (Michael et al., 2009), and equipment design, for both the kayak and the blade (Michael et al., 2009). Racing performance predictions are typically made either by comparison of measurable physiological differences between athletes (Fry and Morton, 1991; Olivier and Coetsee, 2002; van Someren and Palmer, 2003) and/or by extrapolation of laboratory based performance measures on an ergometer (Fry and Morton, 1991). The statistical models used in these studies cannot directly predict the performance changes due to variations of stroke technique or equipment design without recalibrating the model parameters using specific experiments for each new case. Also, they cannot provide insight into the biomechanical causes of varied performance either between athletes with different attributes or for the same athlete with varied equipment. Simulation using biomechanical and fluid dynamics model components may be able to predict these outcomes and better inform athlete training and equipment selection.

Computational simulation of water-based sports presents significant modelling challenges. In kayaking the interactions between the water with the paddle and kayak generate large amounts of momentum, propelling the kayak forwards. In response, the free surface of the water experiences large displacements and fragmentation

(splashing). Smoothed Particle Hydrodynamics (SPH) is a Lagrangian particle method that is well suited to transient fluid problems with moving boundaries of complicated shape. Recent work in swimming (Cohen and Cleary, 2010; Cohen et al., 2011; Cohen et al., 2012) has shown the viability and usefulness of this method for simulation and biomechanical analysis of water-based sports.

We propose a coupled biomechanical-SPH modelling framework for the performance prediction of kayak racing. Three dimensional representations of the kayak and blade geometries and a detailed biomechanical representation of stroke technique are used. In this study we investigate

1. the validity of model outputs;
2. the variation in performance and forces transmitted to the paddle due to variations in stroke rate; and
3. the variation in performance and forces transmitted to the paddle due to two variations in the vertical height of the right stroke (58% and 36% of the original case) through the water;

using generic equipment designs and stroke techniques.

COMPUTATIONAL MODEL

Smoothed Particle Hydrodynamics

Smoothed Particle Hydrodynamics (SPH) is a mesh-free Lagrangian particle method for solving partial differential equations. Fluid dynamics applications of the method are detailed in Monaghan (1994, 2005) and Cleary et al. (2007). Volumes of fluid are represented by a moving set of particles, over which the Navier Stokes equations can be reduced to the following ordinary differential equations:

$$\frac{d\rho_a}{dt} = \sum_b m_b \mathbf{v}_{ab} \cdot \nabla_a W_{ab} \quad (1)$$

where ρ_a is the density of particle a , t is time, m_b is the mass of particle b , where $\mathbf{v}_{ab} = \mathbf{v}_a - \mathbf{v}_b$ and \mathbf{v}_a and \mathbf{v}_b are the velocities of particles a and b . W is a cubic interpolation kernel function that is evaluated for the distance between particles a and b .

$$\frac{d\mathbf{v}_a}{dt} = -\sum_b m_b \left[\left(\frac{P_b}{\rho_b^2} + \frac{P_a}{\rho_a^2} \right) - \frac{\xi}{\rho_a \rho_b} \frac{4\mu_a \mu_b}{(\mu_a + \mu_b)} \frac{\mathbf{v}_{ab} \cdot \mathbf{r}_{ab}}{\mathbf{r}_{ab}^2 + \eta^2} \right] + \mathbf{g} \quad (2)$$

where P_a and μ_a are the local pressure and dynamic viscosity for particle a , η is a small number to mitigate singularities, ξ is a normalisation constant for the kernel function and \mathbf{g} is the gravitational acceleration.

A quasi-compressible formulation of the SPH method is employed. The equation of state for weakly compressible fluids relates the particle density, ρ , and the fluid pressure, P :

$$P = P_0 \left[\left(\frac{\rho}{\rho_0} \right)^\gamma - 1 \right] \quad (3)$$

where P_0 prescribes the overall dynamic pressure scale and the reference density is given by ρ_0 . γ is a material constant, which is equal to 7 for fluids with compressibility properties similar to water.

Nodes of boundary objects are represented as boundary SPH particles, which are repositioned at every time step as a result of any motion and deformation of the boundary. The surface of the athlete's body, the kayak blade and the kayak were specified to move dynamically in all 6 degrees of freedom during each simulation.

Biomechanical model of the athlete and equipment

Dynamic skeletal linkage model of the body

The athlete was represented in the computational model by a deforming surface mesh of a generic male adult. The 3D mesh of 58,000 nodes was rigged to a 23 joint virtual skeleton using the dual quaternion method (Kavan et al., 2008) in Autodesk Maya™ software (Autodesk Inc., San Rafael, CA, USA).

Mesh representations of the kayak and blade

The kayak was represented by a 3D surface mesh of approximately 102,000 nodes. The flat kayak blade was represented as 3D mesh of 1,200 nodes. The blade was kinematically constrained to move with the hands of the athlete to model hand-blade contact. The boundary particle spacing of the blade and the kayak was 10 mm. Zero relative motion between the athlete and the seat of the kayak was assumed. To implement this assumption, the surface mesh of the athlete was attached to the boundary mesh of the kayak using three zero-length springs located in an equilateral triangle, in the horizontal plane at the seat. The stiffness of each spring was 50 kN/m, the sum of which represents the compliance of the soft tissue in the seat of the athlete.

Kinematics digitisation

A symmetric stroke style was digitised from the combination of video footage of an amateur athlete and kinematic data from Limonta et al. (2010). The video footage was split into separate frames at 30 Hz. The rigged surface mesh of the athlete's body was initially positioned in the computational model to match the motion of the athlete for each video frame over one stroke cycle. The motion components in the plane orthogonal to the view in the video footage specified using data from kinematic studies (Limonta et al. 2010) to reflect the stroke style of an elite athlete. The trajectories of the wrists and the tips of the kayak blade are shown in Figure 1. These athlete skeleton kinematics were used to deform the skin mesh and to position the blade at each time in the simulation.

Initial conditions

The initial velocity of the kayak was 2 m/s before paddling began. The tank, initially at rest, was 20 m long, 2 m wide and 1 m deep. The fluid was represented by 5.5M SPH particles with a uniform particle spacing of 20 mm. The viscosity of the water was set as 0.001 Pa·s.

Loading on the blade

Forces imparted on the kayak blade by interaction with the SPH fluid were calculated in global coordinates. Forces were smoothed using a top hat averaging

technique, with a filter width of 10 time increments (of period 0.3 ms). Impulse was calculated per stroke as the integral of force with time. The peak paddle force and the impulse imparted to the water were calculated in the seventh (left hand) and eighth (right hand) strokes.

Variants of stroke rate and style

The stroke rate was varied in the simulation to study its effect on performance. The digitised footage showed the athlete paddling at 95 strokes per minute (SPM). Racing stroke rates are typically 110 to 120 SPM and sprinting stroke rates can be 135 SPM or faster (Baker et al. 1999; Qui et al., 2005). Skeletal kinematics producing rates of 115 and 135 SPM were synthesised using temporal scaling of the digitised motion, to represent racing and sprint stroke styles respectively.

Differences in stroke technique identified between elite and amateur athletes are numerous and inconsistent across a number of studies (e.g. Helmer et al., 2011; Limonta et al., 2010). However, left-right asymmetry of the blade tip trajectory is the most common and significant reported difference. To represent this difference between elite and non-elite athletes, we created two additional sets of stroke kinematics. The depth of the tip of the blade under the water during the right side stroke was reduced by 4.7 cm (to 58% of the original stroke depth) in one case and by 7.2 cm (to only 36% of the original stroke depth) in the other. The left side stroke was left unchanged in both cases. The resulting asymmetric stroke kinematics were used to predict the changes in kayak motion and blade force due to alterations in right side stroke depth.

RESULTS AND DISCUSSION

Symmetrical stroke style at 95, 115 and 135 SPM

Figure 2 shows the predicted forward speed of the kayak for the three stroke rates. The dynamic motion of the kayak is determined by the magnitudes of propulsive force occurring during blade-water interactions and drag forces on the kayak hull (from friction, pressure and wave drag, see Jackson, 1995 and Michael et al., 2009). At the start of each simulation the water is moving slowly relative to the speed of the blade. Because of this large propulsive forces are generated and the kayak speed increases significantly. The kayak speed modestly decreases in between strokes, due to drag forces on the hull. As the speed of the kayak increases, the relative speed between the blade and the water decreases and the propulsive force from the blade-water interaction decreases. When the kayak is moving fast enough, then the propulsive forces will come into equilibrium with drag forces and forward speed reaches equilibrium. For a stroke rate of 95 SPM, equilibrium was reached after the fourth stroke. Equilibrium was not achieved for the 115 SPM and 135 SPM cases within the eight strokes simulated. The forward speed of the kayak after eight strokes increased logarithmically with stroke rate (Table 1). The value for the 135 SPM is consistent with the peak racing speed of elite athletes (Baker et al., 1999).

Peak blade force and impulse during the eighth stroke are also shown in Table 1. The predicted peak forces are consistent with measurements of forces on a flat blade during competitive canoeing (375 N, see Sperlich and Baker, 2000). Peak force increases logarithmically with stroke rate. However, the impulse does not increase strongly with blade force. When the stroke rate increases

the blade interacts with the water for a shorter time. Therefore, whilst blade force increases with stroke rate, the length of time of force transfer is reduced, leading to smaller than linear increases in impulse.

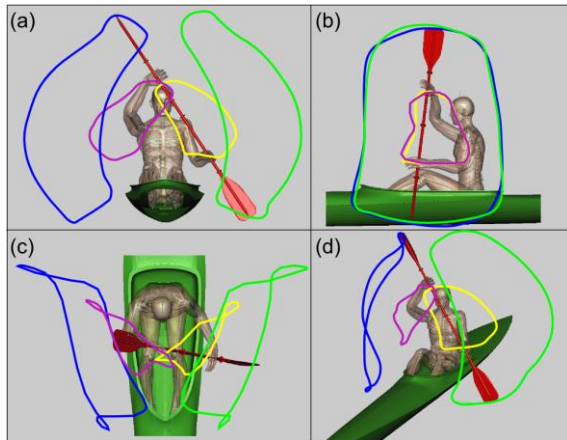


Figure 1: Motion trails of the left and right tips of the kayak blade (blue and green respectively) and the left and right wrist (purple and yellow respectively) from front (a), side (b), top (c) and 3D isometric (d) views.

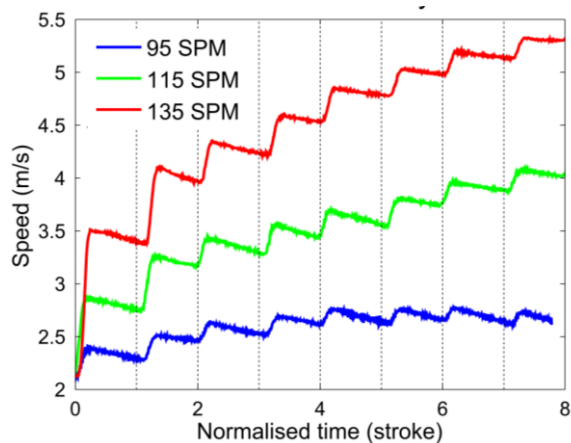


Figure 2: Forward speed versus stroke number over eight stroke cycles, for three stroke rates.

The fluid free-surface behaviour and speed is shown in Figure 3 for two stroke cycles of the 135 SPM case. At the start of the second stroke cycle (1.13 s), the fluid in the bow wave is moving at moderate speed (0.3 m/s). The water in the wake of the kayak is also moving at approximately 0.3 m/s. The fluid near to the hull is dragged along by skin drag forces, with speeds tending to the hull speed as the distance to the hull decreases. As the blade enters the water for the left side stroke the local fluid speeds exceed 0.6 m/s and significant displacement occurs. At the end of the pull phase of the second right stroke (1.27 s) more water than at the catch phase has been violently displaced, resulting in splashing. This surface disturbance has begun to dissipate at the beginning of the right side stroke (1.63 s). Similar behaviour is seen during the catch (1.63 s) and pull (1.80 s) phases of the second left side stroke. During the third stroke cycle (2.00 s to 2.67 s), the speed of the kayak increases further and, as a result, the speed of the fluid in the bow wave has also increased. The amount of disturbance to the fluid surface due to the left side blade entry (2.17 s) is less than for the previous stroke (1.27 s). This is because the kayak is now

closer to its equilibrium speed and the force imparted to the water decreases. Also, the velocities in the water displaced by the present stroke are smaller than in that displaced by the previous stroke. The fluid behaviour during the right side stroke (2.50 s to 2.67 s) has equivalent mirrored attributes to the left side strokes.

The forces imparted to the fluid by the blade and kayak generate 3D vortex structures, which are shown in Figure 4 at three times during the third stroke. As the kayak hull translates forwards, it separates water at the bow and accelerates fluid into a bow wave. Vortices are shed from the front of the kayak as the bow wave is formed. These structures travel with the bow wave, in a backwards direction (relative to the kayak), and become less coherent as they pass its centre. Strong vortices are created when the flow separates from the keel and these interact with vortices formed in the stern wake. Figure 4a shows a large vortex forming as the blade enters the water. As it is removed from the water at the end of the stroke (Figure 4b), this structure has grown in size, primarily in the forward-rear direction. As the athlete prepares for the fourth stroke (0.2 s later, see Figure 4c), this structure is still present, but has translated backwards, relative to the kayak. The large size and lifespan of this structure indicates that a significant amount of energy has been transferred from the blade to the water, as the stroke accelerates the kayak forwards (see Jackson, 1995). Note that whilst the accelerations are smaller as the hull reaches its equilibrium speed (see Figure 2), these structures are still formed (not shown). At equilibrium speed the blade-water interaction forces are smaller and result in smaller, less coherent vortex structures.

Table 1: Forward speed of kayak at the end of the 8th stroke, and peak force and impulse during the 8th stroke for the three simulated stroke rates.

SPH	Speed (m/s)	Peak force (N)	Impulse (Ns)
95	2.6	260	17
115	4.3	350	22
135	5.5	400	23

Symmetric stroke style versus asymmetric variants

Figure 5 shows the forward speed and blade force for the symmetric stroke style and the two increasingly asymmetric stroke styles. The speed increment added to the kayak during the strokes by the right hand decrease with decreasing depth of the paddle stroke. This causes the speed of the kayak after eight strokes to decline with increasing asymmetry (Figure 5, Table 2). However, the speed increment added to the kayak by the left side stroke (which was unaltered in each stroke style) increases with increasing asymmetry of stroke to partially compensate for the weaker increment from the right hand stroke.

Table 2: Forward speed at the end of the 8th stroke and the impulse during the 7th (left) and 8th (right) strokes, for the three stroke styles at 135 SPM.

Case	Speed (m/s)	Impulse (Ns)		
		7 th stroke (Left)	8 th stroke (Right)	7 th + 8 th Stroke
Symmetric	5.5	23	23	46
Asymmetric (58% depth)	5.3	31	12	43
Asymmetric (36% depth)	5.0	37	10	47

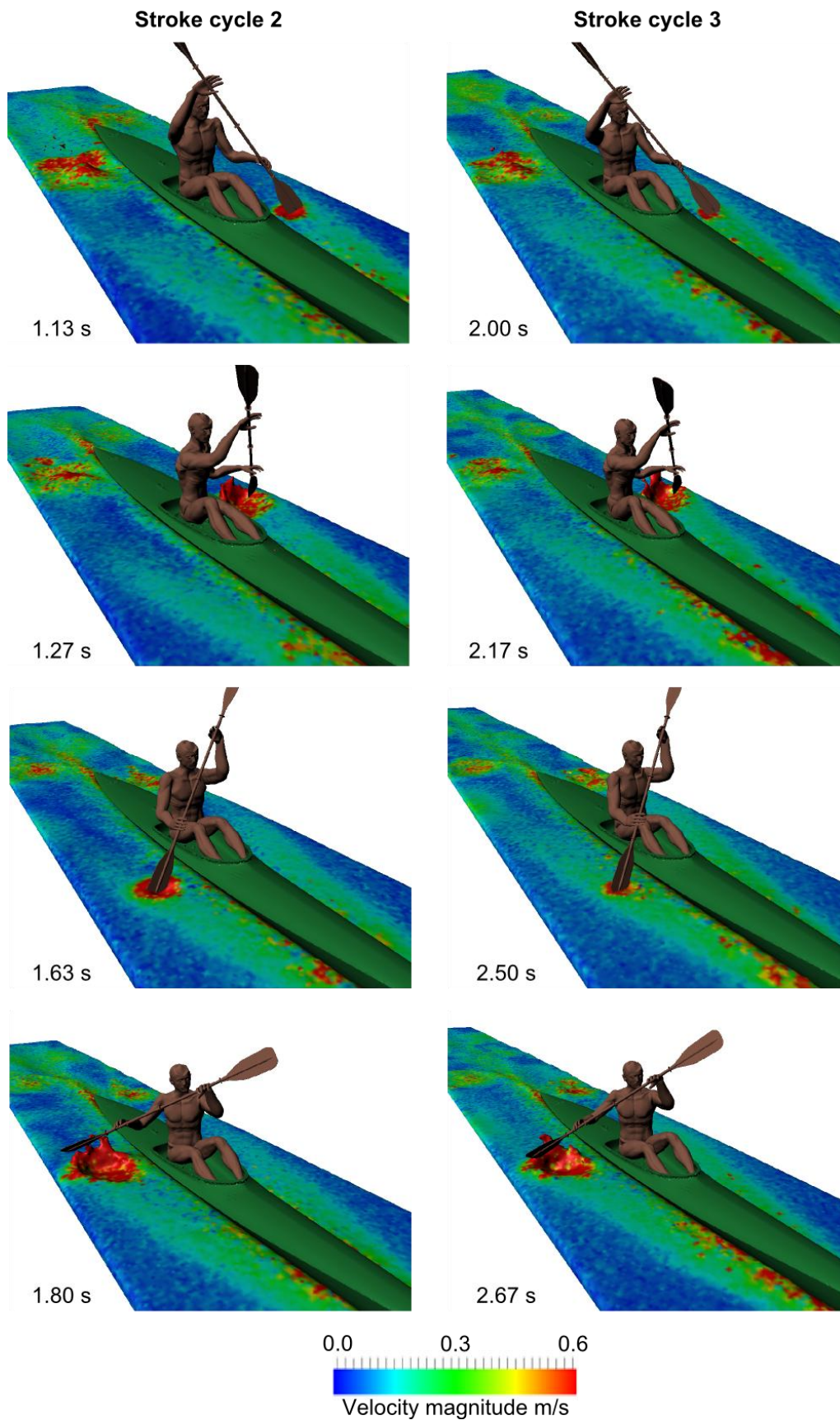


Figure 3: Fluid behaviour during two stroke cycles. The water is coloured by speed and the timing of the image is shown in seconds.

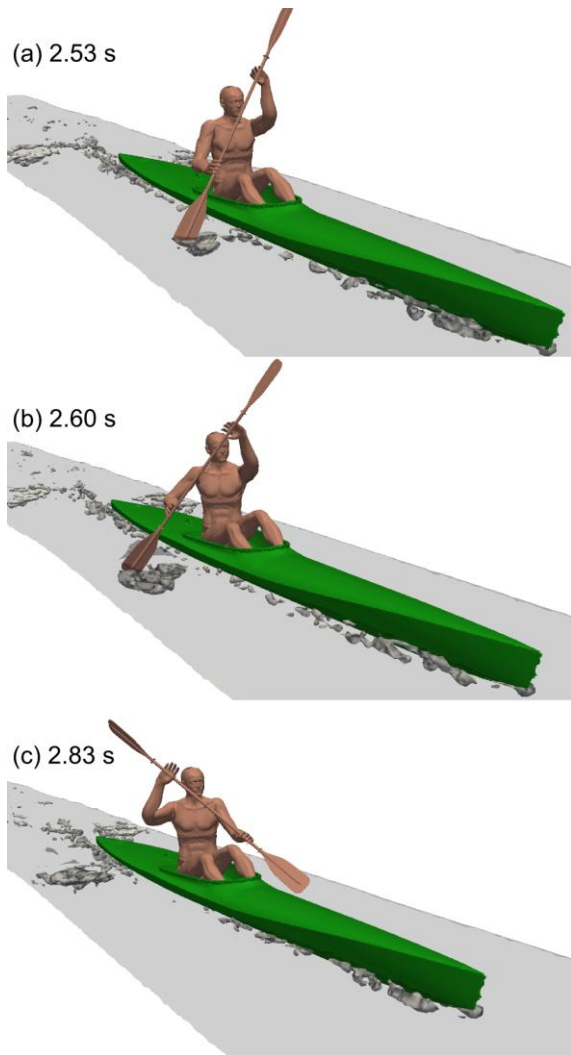


Figure 4: 3D vortex structures shed from the front and rear of the kayak and from the interaction of the blade and water for, the (a) blade catch, (b) blade release and (c) as the athlete prepares for the next (left side) stroke.

The blade force results for both the left and right strokes explain the variations in speed due to increasing stroke asymmetry. Whilst the blade force for the symmetrical stroke style was approximately symmetric for the seventh (left) and eighth (right) strokes, they become increasingly asymmetric as the asymmetry of stroke increases (Figure 5). The force during the left stroke increased with asymmetry to partially compensate for the reduction in the force delivered by the right hand stroke as it decreases. This occurs because the kayak speed is lower at the start of left hand strokes with increasing asymmetry. Lower speed means that the relative speed between blade and water is higher and therefore the propulsive force from the blade-water interaction is larger. So the left hand stroke delivers a larger force and speed increment. This means that the penalty for an asymmetric stroke is partially manifested as a slower average speed but also by higher energy utilisation by the muscles involved in the deeper of the strokes which means a faster rate of fatiguing.

The impulse imparted by the blade (given in Table 2) shows a similar dependence on symmetry of stroke. Impulse was also approximately equal for the left and right strokes of the symmetric stroke case. Again, reflecting the results for blade force, the impulse during the right stroke

decreases with increasing stroke asymmetry and the impulse during the left stroke increases. As mentioned previously, this imbalance in force suggests the likelihood of asymmetric fatigue during racing and indicates that asymmetry in stroke style may be less efficient than a symmetric stroke style.

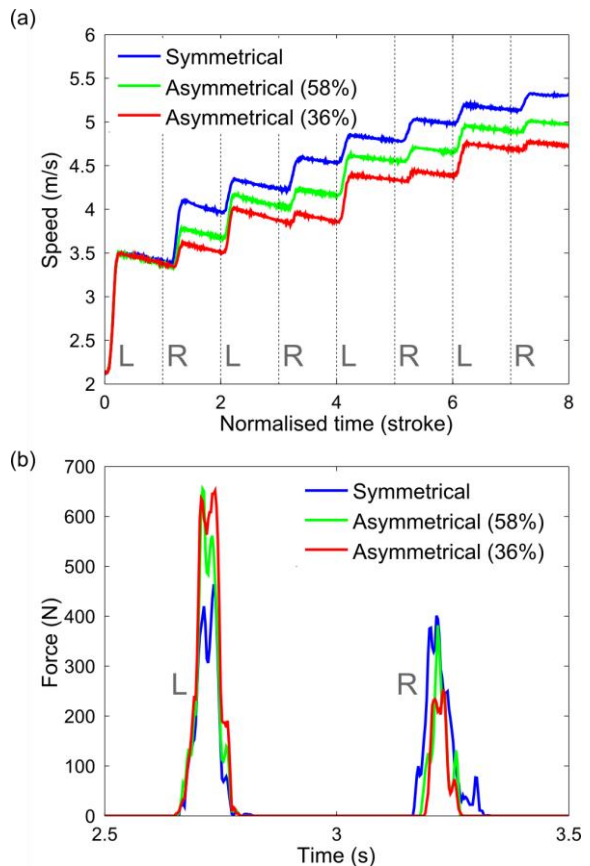


Figure 5: (a) forward speed versus time over eight stroke cycles for three different stroke styles, and (b) magnitude of fluid force on the blade over time for the seventh (L) and eighth (R) strokes for each stroke style. Left side strokes are labelled “L” and right side are labelled “R”.

Future work

Before application to specific athletes, further model validation is required. Resolution studies and variants of fluid tank dimensions will evaluate any dependency of results on initial conditions and simulation parameters. Measures of speed and kinetics can be validated using GPS and strain gauge equipment (e.g. Helmer et al., 2011).

Future applications of the modelling framework can include athlete and equipment specific inputs and calculations of internal biomechanical measures, specifically:

- Individual stroke technique of elite athletes can be determined using 3D motion capture and will be input for starting and steady state conditions. The causes of performance differences between athletes can be studied in greater detail than physical measurements allow.
- Variants of kayak and blade geometries can be used to assess their benefit or cost to performance.
- Evaluations of joint torques, joint powers and muscle forces can be made by inverse dynamics

analysis to determine the strength required to perform a stroke style at a specified speed.

- Predictions of the effects of varied strength and endurance may be made by forward dynamics analysis to inform future training programs of elite athletes.

CONCLUSIONS

In this paper, we have proposed a coupled biomechanical-SPH modelling framework for predicting performance in kayak racing. The framework introduces a number of aspects that have not been modelled in other studies, including

1. Six degrees of freedom motion of the kayak, athlete and blade
2. Free surface fluid dynamics due to kayak motion and blade-water interactions
3. Biomechanical representation of the athlete (skeletal kinematics) coupled to the fluid dynamics solution.

Our results show that realistic racing speed and blade forces can be predicted by the model. Both speed of motion and blade force are consistent with published data.

The forward speed of the kayak was found to increase logarithmically with stroke rate. Peak blade force was also found to increase logarithmically. However, because the time of duration of force transfer between blade and water decreased with increase stroke rate, the impulse imparted during each stroke did not increase to the same degree.

Asymmetry of stroke depth was found to affect the blade force and therefore the speed increment generated by each stroke. When the depth of the right side stroke was reduced, the speed added by the right side stroke decreased. In partial compensation, the speed added by the left side stroke increased. However, the combined effect led to the speed increment per left and right stroke cycle pair decreasing. Similarly, the blade force and impulse decreased for the right side stroke and increased for the left side stroke.

ACKNOWLEDGEMENTS

The authors gratefully acknowledge video footage and technical input from Andrew Eddy, and computational tool development and manuscript review by Dr. Raymond Cohen.

REFERENCES

BAKER, J., RATH, D., SANDERS, R., & KELLY, B. "A Three-Dimensional Analysis of Male and Female Elite Sprint Kayak Paddlers" (1999), *Proceedings of an International Seminar on Kayak-Canoe Coaching and Science, Ghent, Belgium*, 50-66.

BEGON, M., COLLOUD, F. AND SARDAIN, P. (2010), "Lower limb contribution in kayak performance: modelling, simulation and analysis", *Multibody System Dynamics*, **23**, 387-400.

BISHOP, D. (2000), "Physiological predictors of flat-water kayak performance in women", *European Journal of Applied Physiology*, **82**, 91-97.

CLEARY PW, PRAKASH M, HA J, STOKES N, SCOTT C (2007), "Smooth particle hydrodynamics: status and future potential" *Prog Comput Fluid Dy*, **7** (2/3/4):70-90

COHEN, R.C.Z., CLEARY, P.W., (2010), "Computational studies of the locomotion of dolphins and

sharks using Smoothed Particle Hydrodynamics", in: *Proceedings of the 6th World Congress of Biomechanics (WCB 2010)*, IFMBE Proceedings. Springer, Singapore Suntec Convention Centre, pp. 22-25.

COHEN, R.C.Z., CLEARY, P.W., MASON, B.R., (2011), "Simulations of dolphin kick swimming using smoothed particle hydrodynamics". *Hum Movement Sci*, **31**(3), 604-619.

COHEN, R.C.Z., CLEARY, P.W., MASON, B., PEASE, D.L., "Relating kinematics to performance in freestyle swimming using Smoothed Particle Hydrodynamics". *Submitted to Hum Movement Sci June 26 2012*.

FRY, R. W. AND MORTON, A. R. (1991), "Physiological and kinanthropometric attributes of elite flatwater kayakists" *Medicine and science in sports and exercise* **23**, 1297-1301.

HELMER, R. J. N., FAROUIL, A., BAKER, J. AND BLANCHONETTE, I. (2011), "Instrumentation of a kayak paddle to investigate blade/water interactions", *Procedia Engineering*, **13**, 501-506.

JACKSON, P. S. (1995). Performance prediction for Olympic kayaks. *J Sports Sci* **13**, 239-245.

LIMONTA, E., SQUADRONE, R., RODANO, R., MARZEGAN, A., VEICSTEINAS, A., MERATI, G. AND SACCHI, M. (2010), "Tridimensional kinematic analysis on a kayaking simulator: key factors to successful performance", *Sport Sciences for Health*, **6**, 27-34.

MICHAEL, J. S., SMITH, R. AND ROONEY, K. B. (2009), "Determinants of kayak paddling performance", *Sports Biomechanics*, **8**, 167-179.

MICHAEL, J. S., ROONEY, K. B. AND SMITH, R. M. (2012), "The dynamics of elite paddling on a kayak simulator", *Journal of Sports Sciences*, **30**, 661-668.

MONAGHAN JJ (1994), "Simulating free surface flows with SPH", *J Comput Phys* **110**(2), 399-406

OLIVIER, S. C. AND COETSEE, M. F. (2002), "Tests for predicting endurance kayak performance", *S. African J. for Research in Sport, Physical Ed. and Recreation*, **24** (2), 45-54

SPERLICH, J., & BAKER, J. (2000), "Biomechanical testing in elite canoeing", In *Proceedings of the XXth International Symposium on Biomechanics in Sports*, Caceres, Spain, 44-47

QIU, Y., WEI, W., LIU, A., & CAO, J. (2005), "Comparative Research on the Stroke Rhythm of Men and Women Kayakers in the International Competition", *Proceedings of the XXIII International Symposium on Biomechanics in Sport, Beijing, China*, 943-946.

VAN SOMEREN, K. A. and PALMER, G. S. (2003), "Prediction of 200-m sprint kayaking performance", *Canadian journal of applied physiology*, **28**(4), 505-517